Non-adiabatic non-linear impurities in linear hosts

1993 J. Phys.: Condens. Matter 5 8689

(http://iopscience.iop.org/0953-8984/5/46/008)

J. Phys.: Condens. Matter 5 (1993) 8689–8702. Printed in the UK

Non-adiabatic non-linear impurities in linear hosts

D Chen†, M I Molina† and G P Tsironis†‡

† Computational Physics Laboratory, Department of Physics, University of North Texas, Denton, TX 76203, USA

‡ Superconducting Super Collider Laboratory, 2550 Beckleymead Avenue, Dallas, TX 75237, USA

Received 29 June 1993

Abstract. We study the dynamics of non-adiabatic Holstein-type impurities embedded in an infinite linear chain. The impurities are modelled as Einstein oscillators coupled to specific sites of an infinite one-dimensional tight-binding host. We present numerical evidence providing bounds for the onset of self-trapping that depend critically on the initial conditions of the oscillators. We show that, in general, small but finite oscillator masses do not substantially change the self-trapped character of the states. For intermediate as well as large oscillator masses self-trapping can still occur for some initial oscillator preparations.

1. Introduction

One of the means of studying polaron formation and dynamics in deformable media is through the discrete non-linear Schrödinger (DNLS) equation or discrete self-trapping equation [1–3]. The cubic non-linearity terms in the DNLS equation can be seen to arise from an adiabatic-type approximation in the Holstein formulation of the complete polaron problem [2–4]. In the present article we will lift the adiabatic assumption and address numerically the effects that non-adiabatic terms have in the particle dynamics when only a small number of such terms is present in the Hamiltonian. More specifically, we study electronic propagation in the usual tight-binding approximation when one or more Holstein-type impurities are substituted in the linear one-dimensional host. The main motivation for this study comes from recent results in the 'adiabatic' regime that show enhanced electronic propagation in the presence of non-linear impurities [5], in marked contrast with well known conventional substitutional impurity results [6].

We are interested in studying the following set of equations:

$$i\frac{dc_m}{dt} = \epsilon_m c_m + V(c_{m+1} + c_{m-1}) + \alpha \sum_n c_m w_m \delta_{m,n} \tag{1}$$

$$M d^2 w_m/dt^2 + k w_m = -\alpha |c_m|^2 \tag{2}$$

where $c_m(t)$ is the electronic probability amplitude at crystal site m and $w_m(t)$ is the local Einstein oscillator displacement coupled to the electronic level in the same site through the coupling coefficient α. The intersite matrix element V connects the probability amplitudes of site m with its nearest neighbours, ε_m is the local electronic site energy and M and k are the mass and spring constant respectively, of the local Einstein oscillators. The sum on the RHS of the first equation runs over all impurity sites. Note that for $M = 0$ (antiabatic

0953-8984/93/468689+14$07.50

approximation) the local oscillators adjust instantaneously to the electronic presence and for $n = m$ equations (1) and (2) reduce to the DNLS equation with non-linearity parameter $\chi = \alpha^2/k$. In what follows, in order to simplify our calculations and the comparison with the DNLS results we will assume $V = k = 1$ and $\varepsilon_m = 0$. We are therefore left with two parameters to vary, viz. the non-linearity parameter $\chi (= \alpha^2)$ and the inertial mass M of the Einstein oscillators. In the remainder of the article we will use these parameter values and study numerically the evolution that results from (1) and (2) when only a small number of Holstein impurities are present in the host. In section 2 we address the one-impurity problem; in section 3 we study the dynamics from two adjacent impurities embedded in the lattice; in section 4 we comment briefly on the three or more impurities and in section 5 we conclude. We also have a number of analytical results that support the findings of this article; these are included in the appendix.

2. One non-linear impurity

We recently presented exact analytical results for the stationary states of the one-impurity problem in the DNLS equation [5]. In the context of (1) and (2), this case would correspond to $M = 0$ and $n = r$, where r is the (unique) impurity site. We found that there is no bound state at the impurity site for $\chi < 2$. For $\chi > 2$, on the other hand, there is a well defined impurity state formed with energy equal to χ. The point at $\chi = 2$ is therefore a bifurcation point for the system, not dissimilar to that occurring in the stationary states of the non-linear two-site problem [1]. Since the dimer case is fully integrable [1], a complete study of the equations of motion for arbitrary initial conditions is possible [7]. As a result, we know that the dimer undergoes also a 'dynamical self-trapping transition' at $\chi = 4$. The latter occurs for a localized initial condition and it is fundamentally a manifestation (moderately modified by the different initial conditions) of the bifurcation in the stationary states that happens at $\chi = 2$. We can use these well known analytical results to argue that in the case of the non-linear impurity in the infinite chain, the existence of an impurity state for $\chi = 2$ signals the occurrence of dynamical self-trapping at larger χ values. This dynamical bifurcation, even if not found analytically, is bound to occur because of the drastic phase-space change at $\chi = 2$.

2.1. Impurity dynamics for M=0

We performed extensive numerical simulations for one non-linear impurity embedded in the infinite tight-binding chain. We typically chose chains with one hundred sites (in some cases more than five hundred sites) and integrated numerically the differential equations of motion using a well tested fourth-order Runge–Kutta scheme. The natural unit of time is determined by V, which is taken to be equal to unity. We used a time-step equal to 0.002 and a maximum integration time 200–1000. We used only one initial condition, viz. that which places the excitation initially in the impurity site r, and chose as the primary quantity of interest the time-averaged probability of the initially occupied (impurity) site, i.e.

$$\langle P \rangle \equiv \lim_{T \to \infty} \frac{1}{T} \int_0^T |c_r(t)|^2 \qquad |c_r(0)| = 1. \tag{3}$$

An earlier study of the time-averaged probability $\langle P \rangle$ in the context of finite non-linear clusters showed that it is quite sensitive to the occurrence of self-trapping in the dynamics [8]. The numerical results from the calculation of $\langle P \rangle$ as a function of the non-linearity

parameter χ are displayed in figure 1. We note the occurrence of a relatively abrupt change in the time-averaged probability for a critical value χ_c of χ approximately equal to 3.2. This value is compatible with that obtained by Dunlap *et al* [9] using an entirely different numerical approach. The full curve in figure 1 represents a fit to the numerical data by the following functional form:

$$\langle P \rangle = \sqrt{1 - 1/(\chi'/3.2)^2}\,\Theta(\chi' - 3.2) \tag{4}$$

where $\chi' \simeq 1.246\chi - 0.0673$ and $\Theta(x)$ is the step function. The functional form of the fit has been motivated by the exact results for $|c_r|^2$ of [5]. A comparison of these two shows that the shape of the dynamical self-trapping indicator of figure 1 is given very well by the exact stationary state result of [5] only shifted in χ by approximately 1.2. This 'delayed self-trapping' compared to the stationary problem is again similar to the dimer case and it is well understood physically since the stationary states describe the most stable configuration of the system. We note that there is a similar effect in the corresponding linear-impurity problem where, however, the connection between stationary and dynamic quantities is much simpler [6].

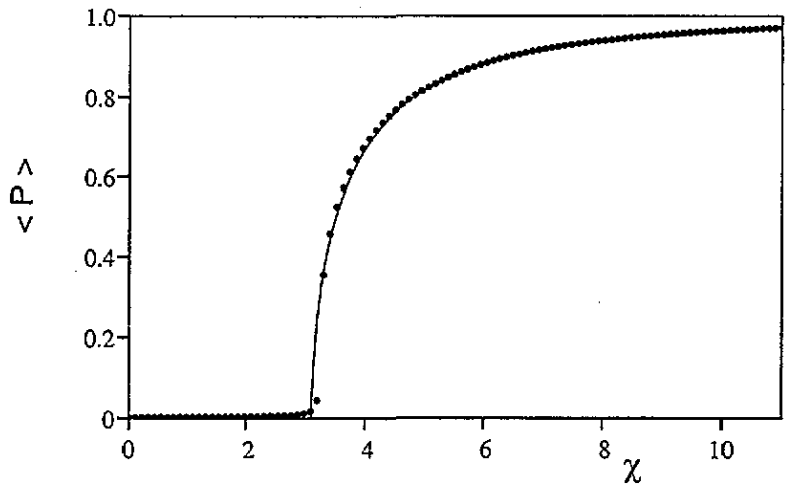

Figure 1. Time-averaged probability at the non-linear impurity site as a function of the non-linearity parameter χ. The points represent actual numerical data and the full curve is the fit to the data by the function of (4). Note the abrupt change in $\langle P \rangle$ signifying the onset of self-trapping.

One of the important quantities that characterizes the self-trapped state is its average extent given by the localization length λ. In order to find the asymptotic localization length for the states in the self-trapped regime, we perform long time simulations in large lattices with non-Hermitian (absorbing) boundary conditions. After the transients disappear, we are left with a localized state that has an approximately exponential (in space) shape around the impurity. We fit this localized state with an exponential and obtain a localization length for different values of the non-linearity parameter. These results as well as a fit to the obtained data are shown in figure 2. We also show, for comparison, the exact localization length obtained from the stationary-state analysis in the same non-linearity parameter range [5]. Note that, for a given χ, the extent of the localized state derived from the stationary state analysis is smaller than that obtained dynamically. This is compatible with the fact that we need more non-linearity to self-trap dynamically rather than in a stationary sense.

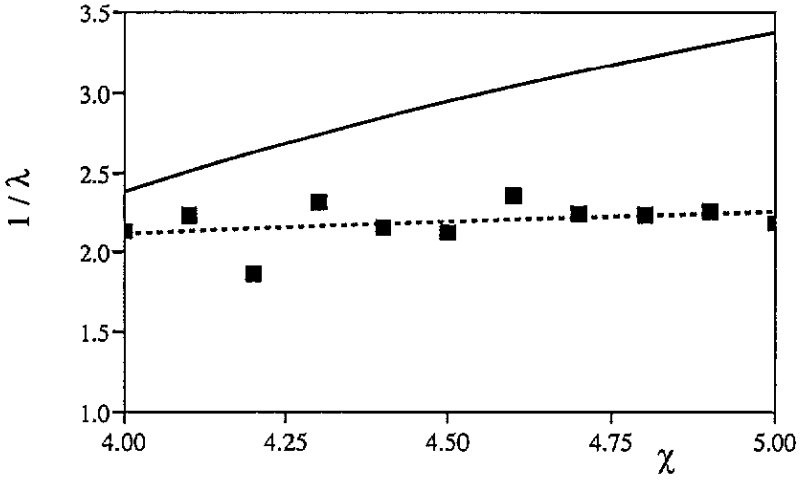

Figure 2. Inverse localization length measuring the extent of the self-trapped state as a function of the non-linearity parameter χ. The squares are numerical data obtained from the asymptotic shape of the localized state created after an initial excitation at the impurity site. The broken line is a fit to these data whereas the full curve is the exact localization length for the stationary state derived in [5]. We note that the localization length obtained from the stationary states is smaller than the corresponding dynamical one.

2.2. *Impurity dynamics for* $M \neq 0$

After investigating the properties of dynamical self-trapping for one impurity in the limit of $M = 0$, we now come to the main issue of this article, viz. the modification of the self-trapping properties when the inertia of the local Einstein oscillator is taken into account. For initial conditions that populate only the impurity site, we solve the equations of motion numerically and evaluate (for long times) the time-averaged probability of occupation of the impurity site, viz. $\langle P \rangle$. The impurity oscillator starts initially from rest with a position determined by assuming complete oscillator relaxation. Since in the limit $M \to 0$, the Holstein oscillator adjusts instantaneously to the presence of the electron at that site, it is natural to assume $w_r(0) = -\alpha$, at least in the small-M regime. Happily, this choice for the initial oscillator position renders the problem easily tractable via regular perturbation theory resulting in modified DNLS equations; this analysis is presented in the appendix. To lowest order in the (small) mass M we obtain the following modified equation for the electron that incorporates the effects of the finite oscillator inertia (A10):

$$\mathrm{i}\mathrm{d}c_m/\mathrm{d}t = V(c_{m+1} + c_{m-1}) - [\chi|c_m|^2 - \sqrt{\chi}M(\mathrm{d}^2/\mathrm{d}t^2)|c_m|^2]c_m\delta_{m,r}. \qquad (5)$$

Note that the inertial effects enter through a second time derivative of the probability at the impurity site in a way that does not affect the stationary-state results of [5].

We present our numerical results in figures 3 and 4. In figure 3(a) we show the time-averaged self-probability $\langle P \rangle$ as a function of the non-linearity parameter χ for various values of the oscillator mass M. It is clear that the dynamical self-trapping transition does indeed survive the presence of a finite time-scale for the oscillator relaxation. We note that for small masses M the change compared to the DNLS case ($M = 0$) is very small. Self-trapping does indeed survive also for larger mass values and with mildly altered characteristics. This behaviour is compatible with the outcomes predicted by the exact

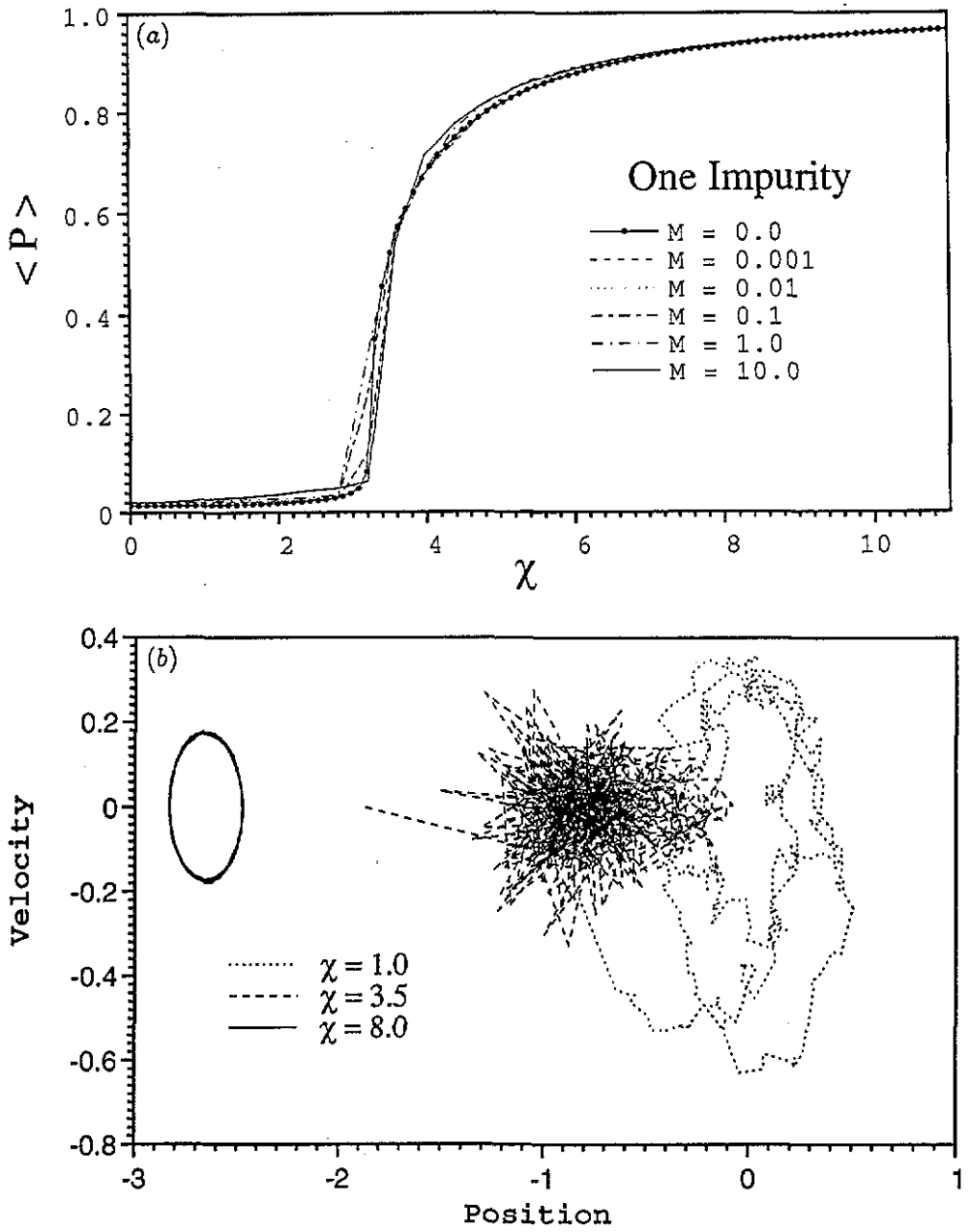

Figure 3. (*a*) Time-averaged probability $\langle P \rangle$ at the impurity site as a function of non-linearity χ for different oscillator masses. The oscillator starts from rest with $w_r(0) = -\alpha$. For small oscillator mass values the self-trapping curve is practically indistinguishable from that for $M = 0$. (*b*) Phase space of the impurity oscillator obtained every oscillator period for three different initial conditions corresponding to three different non-linearity values. Regular oscillations occur in the trapped regime whereas at the transition the oscillator motion is erratic.

equation (5), derived in the limit of small inertial mass. In figure 3(*b*) we show a Poincare surface of section that depicts the phase space of the Einstein oscillator once every oscillator

period for the different cases corresponding to an untrapped electron, while at the transition and for a trapped electron respectively. The shifts of the equilibrium positions are caused by the non-linearity dependence of the initial oscillator position. Note that in the trapped case, the Einstein oscillator executes small-amplitude regular oscillations, whereas in the untrapped case the oscillator is 'squeezed' to a smaller position range. Finally, at the transition, the exchange between the two systems, viz. electron and oscillator, is erratic.

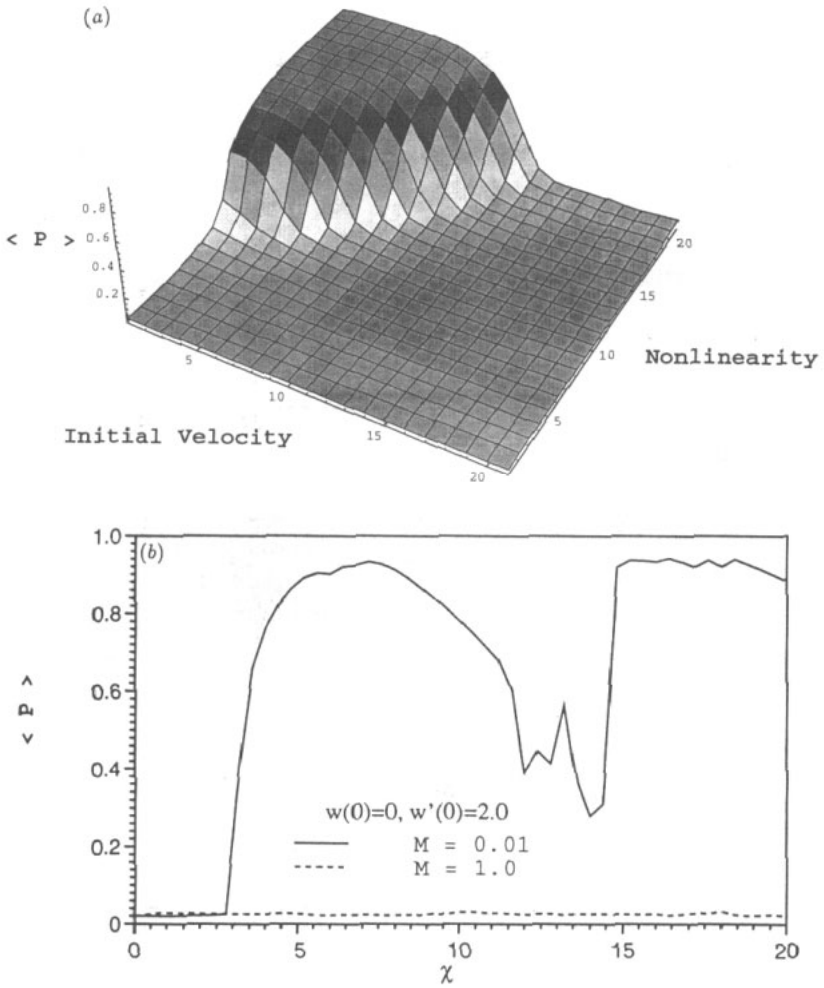

Figure 4. (*a*) Time-averaged probability $\langle P \rangle$ as a function of non-linearity and oscillator initial velocity for $M = 1$. The range on the non-linearity axis is from zero to eight; to obtain the χ value one needs to multiply the numbers on this axis by 0.4. The initial position chosen here is the 'natural' one with initial velocity values given by $(i - 1)/5$, where i is a number on the 'initial velocities' axis. Note that the onset of self-trapping is delayed as the initial velocity increases. (*b*) Time-averaged probability $\langle P \rangle$ as a function of χ for $w_r(0) = 0$ and $w_r'(0) = 2$. Note the 'erratic' behaviour for $M = 0.01$ and the disappearance of the transition for $M = 1$.

In figure 4 we address the influence of the initial conditions of the oscillator on the dynamically self-trapped state. As noted in the appendix, for an initial oscillator position

other than that with $w_r(0) = -\alpha$ (the 'natural' initial condition), the regular perturbation expansion leading to (5) is not valid. This result is readily manifested in the numerical results of figure 4. In figure 4(a) we fix the initial condition of the oscillator to be the 'natural' one and vary the initial momentum of the oscillator. As a result we obtain delayed self-trapping. In figure 4(b), on the other hand, we vary the initial position in addition to changing the momentum of the oscillator itself; we then see the dramatic effects that this change has on the self-trapped state, viz. it can disappear for large enough M. Extensive simulations have shown that the mass value $M \simeq 0.01$ marks the border past which oscillator initial condition effects become very important and the self-trapping transition can disappear. In general, for mass values smaller than approximately 0.01 we have self-trapping for most initial conditions whereas for larger masses we only have trapping for the natural initial condition.

In the limit of large oscillator masses we can use the following modified equation (A15):

$$i\frac{dc_m}{dt} = V(c_{m+1} + c_{m-1}) - \left(\frac{\chi}{M}\int_0^t ds(t-s)|c_m(s)|^2\right)c_m\delta_{m,0}. \tag{6}$$

Note that the effect of the large size of the oscillator mass enters as a time-dependent local site energy that contains all the local probability history convoluted in time. This term does not provide any assistance to self-trapping since in the time-scale in which it is effective, the much faster electron has already escaped in the crystal. Our numerical simulations confirm this tendency, viz. there is no self-trapping in the limit of large oscillator mass except for initial oscillator positions that are different from zero. The latter case, however, is trivial since this probability localization is a linear effect.

3. Two non-linear impurities

The numerical results from the study of the self-trapped properties of the two Holstein impurities placed in adjacent sites and embedded in the linear chain are shown in figures 5–7. We use again an initial condition that places the electron completely on one site of the two-site non-linear system with the corresponding oscillator starting from rest with the same displaced initial position as used in section 2. From figure 5 we observe that when the non-linear dimer ($M = 0$) is embedded in the infinite linear chain, dynamical self-trapping still occurs for a χ value close to four. We note, however, the presence of a 'precursor' to this transition occurring for χ values close to three. This behaviour arises from the single-impurity results discussed previously. For a particle placed initially on one of the two possible non-linear sites, the system does not have sufficient non-linearity for $\chi < 4$ to 'recognize' its neighbouring site as a non-linear one and a self-trapped state compatible with only one non-linear impurity begins to form. Further increase of χ, however, strengthens the participation of the initially non-occupied site and as a result probability flows from the initially occupied to the other non-linear site. Only for strong enough non-linearity does a genuine self-trapped state form for a χ value close to the isolated dimer case [7]. For $M \neq 0$ the situation does not change substantially for most mass values. We observe that for small masses the time-averaged probability is almost indistinguishable from the corresponding one for $M = 0$. We notice, however, that when the oscillator mass becomes very large the precursor phenomenon begins to disappear while, at the same time, the main self-trapping phenomenon remains. In figure 6 we present the actual time dependence of the evolution of the two non-linear sites together with their sum, representing the total non-linear cluster

probability. Complete switching of the probabilities between the two sites occurs at $\chi = 4$ (figure 6(*b*)). This is clearly a manifestation of the sensitive dependence of self-trapping on the participation of the rest of the crystal. Finally, in the limit of very large masses, with initial oscillators completely at rest, we observe no transition at all. This is compatible with the results obtained in the previous section for one impurity. In order to demonstate the sensitivity of the phenomena discussed on initial oscillator conditions we show in figure 7 the average probability plot for the two-impurity case, when *both* oscillators are displaced equally. For small oscillator masses the changes compared with the previous case are minimal. However, as the oscillator mass exceeds a value $M \simeq 0.01$, the characteristics of the self-trapped state change substantially especially for larger non-linearity values. We note that, in addition to the windows of substantially reduced trapping, we have, for larger oscillator masses, complete destruction of the self-trapped state, at least for the non-linearity values displayed in figure 7. As the mass of the Einstein oscillators increases, the oscillator time-scale reduces and for $M = 1$ becomes identical to the electronic time-scale. For this value, there seems to be a resonant coupling between the two subsystems leading to a substantial delay in the occurrence of localization. It is noteworthy that both cases of $M = 0.1$ and $M = 100$ lead to destruction of the localized state and escape of most of the initial probability to the linear lattice (at least for all non-linearity values shown in figure 6) whereas for $M = 1$ self-trapping does indeed occur. The occurrence of 'antitrapping windows' as in the case of $M = 0.01$ is related to the sensitive dependence of the system on initial preparation as well as the resonant escape of probability from the non-linear cluster for some non-linearity parameter values.

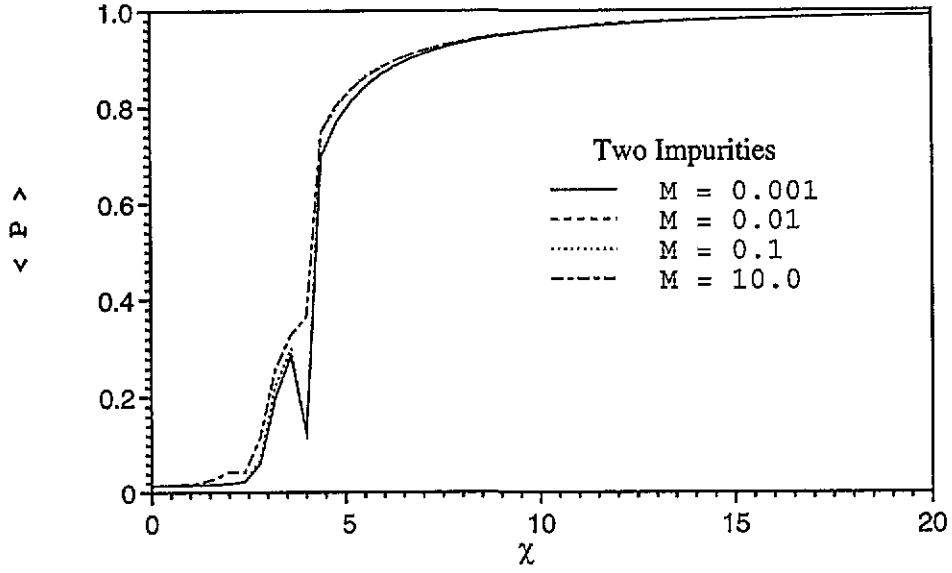

Figure 5. Time-averaged probability (P) for the initially occupied site of a two-site non-linear cluster as a function of the non-linearity parameter χ for different oscillator mass values. The oscillator corresponding to the initially occupied site is initially displaced. Self-trapping features do not change substantially from the $M = 0$ case. The curve for the latter is indistinguishable from that for $M = 0.001$.

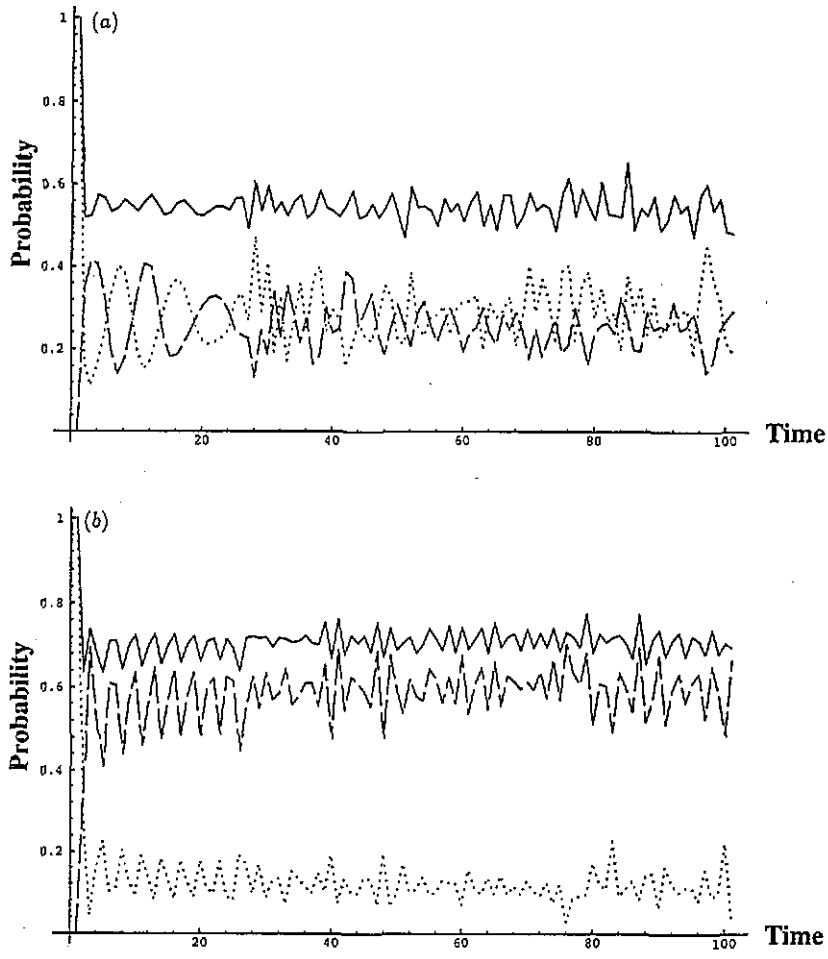

Figure 6. Time dependence of the probability of both non-linear sites as well as their sum (total cluster probability) for $M = 0.001$. (*a*) $\chi = 3.6$: both non-linear sites share approximately the same amount of probability. (*b*) $\chi = 4$: almost all the cluster probability accumulates in the initially non-occupied site. Full curves represent the sum of the impurity site probabilities, dotted curves the initially occupied site and broken curves the initially unoccupied site respectively.

4. Many non-linear impurities

We have also performed extensive simulations for small Holstein chains with three, four, etc consecutive impurity sites embedded in the infinite chain. We used initial conditions that place the particle initially either at one end of the impurity segment or in its centre. The largest value of χ used was 20 and the largest oscillator mass was $M = 100$. For this range of values we observed that the tendencies realized in the dimer persist, viz. there is in general dynamical self-trapping for oscillators with finite inertia, especially when the latter is very small. The occurrence of self-trapping depends not only on the initial oscillator positions but also on which impurity site is initially excited (figure 8). For initial conditions different from the 'natural' ones, self-trapping ceases for mass values larger than 0.01, with the latter value being a borderline case as in the two-impurity case. In the cases when self-trapping occurred, i.e. for mass values approximately less than 0.01, the transition occurred

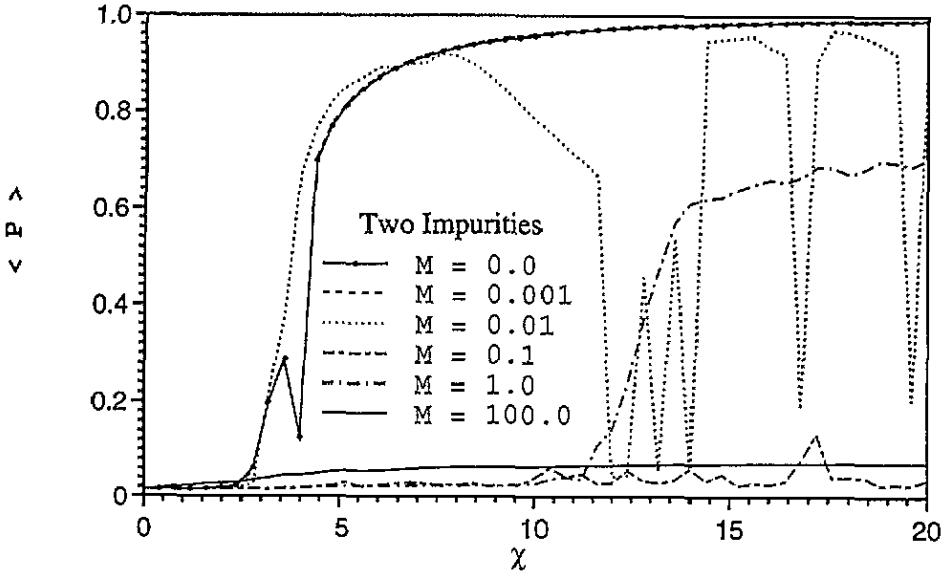

Figure 7. Time-averaged probability of the initially occupied site as a function of χ for a two-site system embedded in the chain. Both oscillators have been initially shifted equally. The self-trapping properties of the system change drastically for mass values larger than approximately 0.01.

for $\chi \simeq 4$, a value that is compatible with the findings of [8]. The case of a cluster with three Holstein impurities is depicted in figure 8.

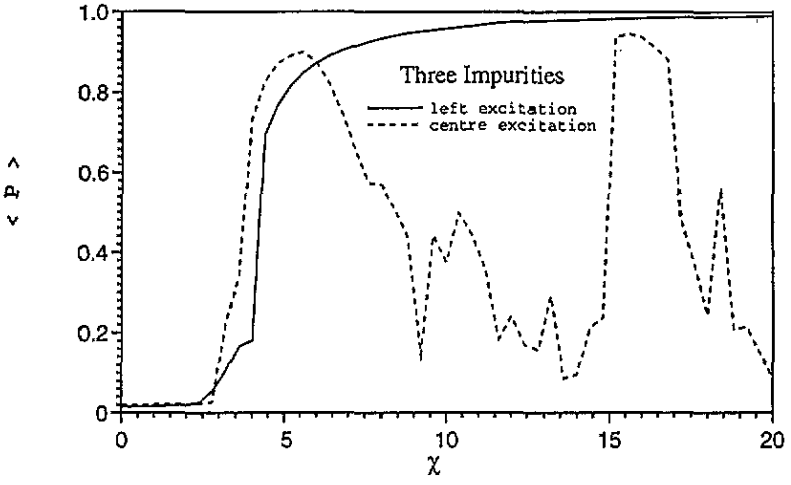

Figure 8. Time-averaged self-trapping probability for a cluster of three non-linear sites. When the central site is initially excited the behaviour becomes erratic. The oscillator mass is $M = 0.01$ and we displace the oscillator in the initially occupied site.

5. Conclusions

We have presented a numerical study of the effects of finite inertia in the non-linear properties of DNLS-like impurities embedded in a one-dimensional linear lattice. The motivation for this work was twofold: (a) to address the issue of the survival of self-trapping in situations where the 'antiabatic' approximation has not been invoked and (b) to provide a framework for the further understanding of electron motion in substitutional disordered systems, when the impurities involve a strong local electron–phonon coupling. We modelled our impurities by simple Einstein oscillators and coupled them to the electronic problem with a linear coupling in the spirit of Holstein. We did not include damping, or stochastic fluctuations, as was done in earlier works in the context of the non-linear dimer model [10]. By varying the mass of the Einstein oscillators we directly influenced the time-scale of the vibrational subsystem relative to the electronic problem; this would not have been possible if damping and fluctuations had been added in the oscillator. For oscillator mass $M = 0$, we recover exactly the DNLS-like impurity embedded in the infinite chain, whereas as the oscillator mass becomes non-zero inertia effects come directly into play. The mathematical problem of such mass variation departing from the limit of $M = 0$ is, in general, addressed through singular perturbation methods; these, however, become exceptionally difficult for an undamped equation such as (2). Fortunately, the initial condition of fast lattice relaxation to an initially localized electron transforms the problem into one of regular perturbation, leading to an asymptotic series solution of (2). As a result, new modified DNLS-like equations for the one-impurity problem can be derived. For a small mass M, the lowest-order correction term is proportional to the second time derivative of the impurity site occupation probability (5). This equation is conspicuously similar to a modified NLS equation derived in [2] in the context of the Davydov soliton problem. In the other oscillator mass limit, viz. for $M \to \infty$, the oscillator system is infinitely slower than the electron system. The choice of an appropriate initial condition for the oscillator, viz. that of complete initial rest in its equilibrium position, results, to the lowest order in $1/M$, in an equation that contains a time convolution correction term (6).

The basic findings of this aritcle can be summarized as follows: (i) The self-trapping properties of the impurities depend strongly on the initial oscillator conditions. The 'natural' initial conditions are, in the small-mass limit, those with an oscillator that starts from rest and is displaced due to the presence of the electron in that site. In the other extreme of large oscillator mass, the natural initial condition is that of an undisplaced oscillator. These initial conditions bypass the initial layer problem and give rise to modified equations for the electron, such as (5) and (6). (ii) For small mass M, dynamical self-trapping survives in the presence of finite inertia for one or more Holstein impurities embedded in a chain. The critical self-trapping values do not change drastically from that in the $M = 0$ case. The characteristic length scale introduced by the presence of a localized state remains approximately the same with that in the $M = 0$ case. (iii) For initial conditions other than the natural ones (in the small-mass limit) the self-trapped state survives for oscillator mass values less than $M \simeq 0.01$. For the latter value, the system behaves in an 'erratic' way with windows of antitrapping in the middle of the self-trapped region. For larger mass values self-trapping does not occur at all with one notable exception, viz. the region near $M \simeq 1$. In this regime the oscillator and electronic problems have identical frequencies and as a result there is self-trapping but for larger χ values. (iv) Regular perturbation theory can be used to derive approximate modified non-linear equations to study these phenomena. (v) When the oscillator mass is very large, initial conditions different than the natural ones (for that limit) show some probability localization. This is a purely linear effect resulting from

the effectively linear impurity that these initial conditions introduce in the lattice. Finally, we should point out that some of the present findings, viz. the survival of self-trapping for small oscillator masses, contradict results presented in [11] that address a similar, but not identical, problem. Additional work is necessary for complete understanding of the nature of the self-trapped states.

Appendix

When there is only one Holstein-type impurity at site $m = r = 0$ of the linear host, (1) and (2), using the conventions discussed previously, become

$$\mathrm{i}\,\mathrm{d}c_m/\mathrm{d}t = V(c_{m+1} + c_{m-1}) + \sqrt{\chi}\,y c_m \delta_{m,0} \tag{A1}$$

$$M\mathrm{d}^2y/\mathrm{d}t^2 + y = -\sqrt{\chi}|c_0|^2 \tag{A2}$$

where we designate the displacement of the Einstein oscillator with y. For $M = 0$, (A2) is trivially solved and upon substitution into (A1) we recover the DNLS equation. In order to investigate analytically what happens for small but non-zero values of M we need first to solve (A2) in that limit. Let us designate $M \equiv \varepsilon$, where ε is a small positive number and with $y(t, \varepsilon)$ the complete solution of (A2) that depends on the value of ε:

$$\epsilon\mathrm{d}^2y(t,\epsilon)/\mathrm{d}t^2 + y(t,\epsilon) = F(t) \equiv -\sqrt{\chi}|c_0(t)|^2 \tag{A3}$$

It is straightforward to see that the solution of (A3) presents a singular perturbation problem *except* for the unique initial condition $y(0) = F(0)$. We can see this from the exact solution of (A3) for the case of $y'(0) = 0$, i.e.

$$y(t,\epsilon) = y(0)\cos\frac{t}{\sqrt{\epsilon}} + \frac{1}{\sqrt{\epsilon}}\int_0^t \mathrm{d}t' \sin\frac{t-t'}{\sqrt{\epsilon}}F(t'). \tag{A4}$$

After some trivial reorganization, (A4) can be rewritten as

$$y(t,\epsilon) = \left(y(0) - F(0) - \int_0^t \mathrm{d}t' \sin\frac{t'}{\sqrt{\epsilon}}F'(t')\right)\cos\frac{t}{\sqrt{\epsilon}} + F(t) - \sin\frac{t}{\sqrt{\epsilon}}\int_0^t \mathrm{d}t' \sin\frac{t'}{\sqrt{\epsilon}}F'(t') \tag{A5}$$

with $F'(t)$ being the time derivative of $F(t)$. We note that in the limit $\varepsilon \to 0$, the integral terms in (A5) average out to zero (except under very singular circumstances not realizable in our problem) and we are left with the following terms:

$$\lim_{\epsilon\to 0} y(t,\epsilon) = F(t) + \lim_{\epsilon\to 0}[y(0) - F(0)]\sin\frac{t}{\sqrt{\epsilon}}. \tag{A6}$$

Thus, for $y(0) = F(0)$, as ε approaches zero, $y(t, \varepsilon) \to y(t, 0)$, for all t and for this exceptional initial condition there is no need to worry about the initial layer problem [12]. We note that the aforementioned initial condition is the 'natural' one since it corresponds physically to an infinitely fast relaxation of the lattice to the presence of the initial excitation

at site $m = 0$. We can now use regular perturbation theory and express the solution of (A3) with an asymptotic series expansion of powers of ε [12]

$$y(t, \epsilon) \simeq \sum_{l=0}^{\infty} y_l(t)\epsilon^l. \tag{A7}$$

Direct substitution of (A7) into (A3) leads to a set of equations (with their corresponding initial conditions) for different orders in ε. For $\varepsilon = 0$ we recover

$$y_0(t) = F(t) \qquad y_0(0) = F(0) \equiv -\sqrt{\chi} \qquad y_0'(0) = 0 \tag{A8}$$

whereas to order ε^l, for $l > 0$, we have

$$y_l'' + y_{l-1} = 0 \qquad y_l(0) = y_l'(0) = 0. \tag{A9}$$

To lowest order then in ε, (A1) then becomes

$$\mathrm{i}\mathrm{d}c_m/\mathrm{d}t = V(c_{m+1} + c_{m-1}) - [\chi|c_m|^2 - \sqrt{\chi}\epsilon(\mathrm{d}^2/\mathrm{d}t^2)|c_m|^2 + \ldots]c_m\delta_{m,0} \tag{A10}$$

where the additional terms are higher-order (even) derivatives of the probability at site m, each entering at a higher order in ε. For a small impurity mass ε, the contribution to the local site energy of the additional term on the RHS of (A10) is quite small, especially since it involves the second derivative of a relatively slowly varying function. In light of this, it is clear why the self-trapping properties of the one-impurity problem do not change substantially for small masses, as was shown in section 2.2 (figure 3). On the other hand, when the initial conditions of the Einstein oscillator change, the critical values for dynamical self-trapping vary considerably. These values are directly influenced by the singular aspect of the initial layer problem for the oscillator that becomes effective for initial conditions different than the 'natural' one. These effects are manifested predominantly in the two- or more-impurity problems.

Let us now briefly discuss the opposite oscillator limit, i.e. when the mass M becomes very large. Denoting $M = 1/\delta$, with δ small, (A2) becomes

$$\mathrm{d}^2y(t, \delta)/\mathrm{d}t^2 + \delta y(t, \delta) = \delta F(t) \equiv -\delta\sqrt{\chi}|c_0(t)|^2. \tag{A11}$$

When $\delta = 0$, the time-scale of the electron is infinitely faster than that of the oscillator and the solution of (A11) is trivial. For an oscillator initially at rest we simply have $y(t) = y(0)$. Substitution of this solution back into (A1) leads to a completely linear electron problem with one linear defect with local energy proportional to $y(0)$. As a result, in this limit, linear trapping occurs [6] for $y(0) \neq 0$. However, since it takes an infinite amount of time for the information of the presence of an initially localized electron to pass to the oscillator, it is natural to assume that in this regime $y(0) = 0$. Thus, an infinitely 'sluggish' oscillator initially at complete rest does not affect the motion of the electron. For δ small but non-zero we can use an asymptotic expansion in δ, similar to that of (A7) and obtain

$$y_0''(t) = 0 \qquad y_0(0) = 0 \qquad y_0'(0) = 0 \tag{A12}$$

$$y_1'' + y_0 = F(t) \qquad y_1(0) = y_1'(0) = 0 \tag{A13}$$

$$y_l'' + y_{l-1} = 0 \qquad y_l(0) = y_l'(0) = 0 \qquad \text{for } l \geqslant 2. \tag{A14}$$

After solving (A12) and (A13) and substituting into (A2) we obtain to lowest order in δ

$$i\frac{dc_m}{dt} = V(c_{m+1} + c_{m-1}) - \left(\chi\delta \int_0^t ds(t-s)|c_m(s)|^2 + \dots\right)c_m\delta_{m,0}. \quad \text{(A15)}$$

We note that the effect of the finite mass of the Einstein oscillator appears now to be a convolution in time of the site probability that modifies the 'impurity' term of (A15) by including the complete history of the electronic probability at that site. From a comparison of (A10) and (A15) we observe the different nature of the correction terms arising from the finite value of the oscillator mass in the two extremes. When the oscillator is fast compared to the electron, the lowest-order correction is proportional to the second time derivative of the impurity site probability whereas in the opposite limit of slow oscillator–fast electron the correction enters as a convolution over the entire history of the impurity probability.

References

[1] Eilbeck J C, Lomdahl P S and Scott A C 1985 *Physica* D **16** 318

[2] Lindenberg K, Brown D W and Wang X 1988 *Lecture Notes in Physics* ed L Garrido (New York: Springer)
Wang X, Brown D W and Lindenberg K 1989 *Phys. Rev.* B **39** 5366

[3] Kenkre V M 1989 *Disorder and Nonlinearity* ed A Bishop *et al* (New York: Springer) and references therein

[4] Holstein T 1959 *Ann. Phys., NY* **8** 325

[5] Molina M I and Tsironis G P 1993 *Phys. Rev.* B **47** 15 330
Molina M I and Tsironis G P, in preparation

[6] Economou E N 1979 *Green's Functions in Quantum Physics (Springer Series in Solid State Sciences 7)* (Berlin: Springer)

[7] *Kenkre V M and Campbell D K 1986 Phys. Rev.* B **34** *4959*
Kenkre V M, Tsironis G P and Campbell D K 1987 *Nonlinearity in Condensed Matter Physics* ed A R Bishop *et al* (Berlin: Springer)
Tsironis G P and Kenkre V M 1988 *Phys. Lett.* **127A** 209

[8] Molina M I and Tsironis G P 1993 *Physica* D **66** 135

[9] Dunlap D H, Kenkre V M and Reineker P 1992 *Phys. Rev.* B **47** 14 842

[10] Kenkre V M and Wu H-L 1989 *Phys. Rev.* B **39** 6907; 1989 *Phys. Lett.* **135A** 120
Grigolini P, Wu H-L and Kenkre V M 1989 *Phys. Rev.* B **40** 7045

[11] Vitali D, Allegrini P and Grigolini P 1993 *Chem. Phys.* (special issue on Dissipative Dynamics) ed N Agmon and D Levine, to appear

[12] O'Malley R E 1991 *Singular Perturbation Methods for Ordinary Differential Equations* (New York: Springer)